AD

METHODS OF PREDICTING BLAST LOADS INSIDE AND BLAST FIELDS OUTSIDE SUPPRESSIVE STRUCTURES

ADA024906

by
W. E. Baker
P. S. Westine

November 1975
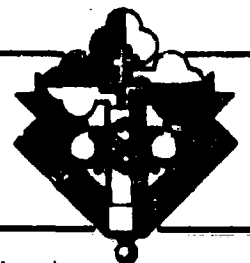
SOUTHWEST RESEARCH INSTITUTE
Post Office Drawer 28510, 8500 Culebra Road
San Antonio, Texas 78284

D D C

MAY 26 1976

B

DEPARTMENT OF THE ARMY
Headquarters, Edgewood Arsenal
Aberdeen Proving Ground, Maryland 21010

REPORT DOCUMENTATION PAGE

READ INSTRUCTIONS
BEFORE COMPLETING FORM

1. REPORT NUMBER EM-CR-76026	2. GOVT ACCESSION NO.	3. RECIPIENT'S CATALOG NUMBER

4. TITLE *(and Subtitle)* METHODS OF PREDICTING BLAST LOADS INSIDE AND OUTSIDE SUPPRESSIVE STRUCTURES	5. TYPE OF REPORT & PERIOD COVERED Technical Report no. 5, Jan — Sep 74
	6. PERFORMING ORG. REPORT NUMBER Report No. 5

7. AUTHOR(s) W. E. Baker P. S. Westine	8. CONTRACT OR GRANT NUMBER(s) DAAD05-74-C-0751 DAAA05-75-C-0083

9. PERFORMING ORGANIZATION NAME AND ADDRESS Southwest Research Institute P. O. Drawer 28510 San Antonio, Texas 78284	10. PROGRAM ELEMENT, PROJECT, TASK AREA & WORK UNIT NUMBERS DARCOM - PA/A-4032, DARCOM — 5741264

11. CONTROLLING OFFICE NAME AND ADDRESS Commander, Edgewood Arsenal Attn: SAREA-TS-R Aberdeen Proving Ground, Maryland 21010	12. REPORT DATE November 1975
	13. NUMBER OF PAGES 19

14. MONITORING AGENCY NAME & ADDRESS *(if different from Controlling Office)* Commander, Edgewood Arsenal Attn: SAREA-MT-H Aberdeen Proving Ground, MD 21010 (CPO Mr. Bruce W. Jezek 671-2661)	15. SECURITY CLASS. *(of this report)* UNCLASSIFIED
	16a. DECLASSIFICATION/DOWNGRADING SCHEDULE NA

16. DISTRIBUTION STATEMENT *(of this Report)*

Approved for public release; distribution unlimited.

17. DISTRIBUTION STATEMENT *(of the abstract entered in Block 20, if different from Report)*

18. SUPPLEMENTARY NOTES

19. KEY WORDS *(Continue on reverse side if necessary and identify by block number)*

Blast loading	Effective vent areas
Internal blast pressures	Quasi-static pressures
Blast attenuation	Venting times
Blast scaling	Suppressive shields

20. ABSTRACT *(Continue on reverse side if necessary and identify by block number)*

This report presents methods for predicting blast loads, quasi-static pressure rises, and venting times within suppressive structures. In addition, side-on pressures outside these vented structures are estimated. Data are presented in scaled form.

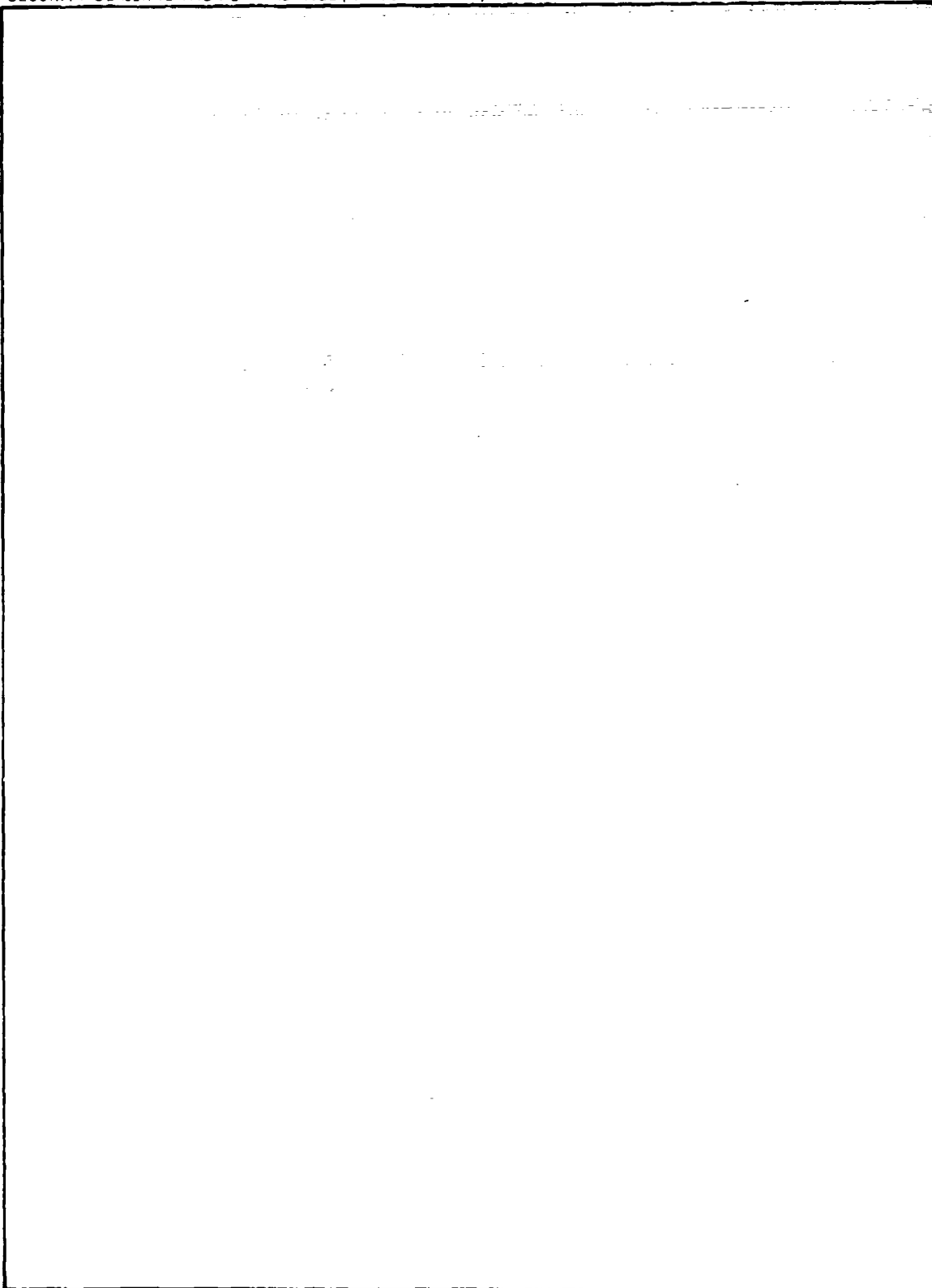DD $_{1\ JAN\ 73}^{FORM}$ 1473   EDITION OF 1 NOV 65 IS OBSOLETE

328 200

SUMMARY

Methods have been developed for predicting the blast loads, quasi-static pressure rise, and duration of the quasi-static pressure rise within a suppressive structure. In addition, the side-on overpressures outside a vented suppressive structure are estimated.

Before any prediction procedure could be developed, the effective vented area ratio $(\alpha_{eff} = A_{vent}/A)$ for a multiwalled structure with various size vents in each wall had to be developed. This relationship was assumed, and then employed in a model analysis to develop pi terms for predicting loads and durations inside the structure as well as overpressures outside the structure. Finally, experimental test data taken from the literature were used to develop functional relationships. Whereas in the past, investigators have assumed that the influence of a vented suppressive structure was a reduction in effective charge weight, this solution shows that a more accurate concept is the creation of an effective standoff distance less than the free-field standoff distance at which blast pressures are the same for a given size energy release. This effective standoff distance is a function of the effective vented area ratio α_{eff}, the free-field standoff distance for a given overpressure, and the width of a suppressive cubical structure. Data from a variety of test structures show that the procedure predicts outside pressures to within one standard deviation of 18.6%.

For the vast majority of suppressive structures, the quasi-static pressure rise within the structure is independent of the vented areas. Test data indicate that provided $(\alpha_{eff}A)^{3/2}/V$ is less than 0.0775, the maximum internal quasi-static pressure is a function only of the charge weight divided by the volume because the maximum pressure is reached before insignificant venting occurs.

This report is a reprint of a paper presented at the 16th Explosive Safety Seminar, Hollywood Beach, Florida, September 1974.

PREFACE

TABLE OF CONTENTS

Page

LIST OF ILLUSTRATIONS

METHODS OF PREDICTING BLAST LOADS INSIDE AND
BLAST LOADS OUTSIDE SUPPRESSIVE STRUCTURES

I. INTRODUCTION

The loading from an explosive charge detonated within a vented or unvented structure consists of two almost distinct phases. The first phase is that of reflected blast loading. It consists of the initial high pressure, short duration reflected wave, plus perhaps several later reflected pulses arriving at times closely approximated by twice the average time of arrival at the chamber walls. These later pulses are attenuated in amplitude because of irreversible thermodynamic process, and they may be very complex in waveform because of the complexity of the reflection process within the structure, whether vented or unvented. If the structure has solid walls, the blast loading can be estimated by using sources of compiled blast data for normally reflected blast pressures and impulses such as References 1 and 2, and the well-known Hopkinson's blast scaling law (see Chapter 3 of Ref. 3). The effect of vented panels in the suppressive structures on reduction of the reflected blast loading can be very complex, and will not be addressed in detail in this paper.

As the blast waves reflect and re-reflect within the structure and as unburned detonation products combine with the available oxygen,* a quasi-static pressure rise occurs and the second phase of loading takes place. Proctor and Filler[4] present some data on thse pressures, Proctor[5] has developed a computer program to calculate both blast and quasi-static pressure rises, and Sewell and Kinney[6] also present methods for estimating this later phase. In addition, Keenan and Tancreto[7, 8] have made measurements of blast pressures emitted from rectangular box cubicles with various vent areas and pressure rises within the cubicles. Finally, Lasseigne[9] has measured static pressure rises in closed chambers to obtain design information for a specific suppressive structure. From these references, one obtains the answer that for the particular ratios of vent area to chamber volume tested, the venting has no effect on the peak quasi-static pressure. Thus, peak static pressures for unvented or poorly vented structures are the same. Unfortunately, essentially no data exist for quasi-static pressures within well-vented structures and the crucial question of the actual maximum pressure rise within such chambers remains unanswered. We must at present use the unvented pressure rise for design purposes. We have, however, conducted a model analysis and fitted curves to all data available to date to obtain the best possible estimate of this pressure. The model analysis and curve fits are presented later in this report.

A third important question regarding blast loading and suppressive structures is, "Can blast pressures outside these structures be predicted for specific designs?" Many of the past measurements of effectiveness of these structures have been based on blast attenuation which they provide (see Refs. 9-12). Using these references and more recent data from MTF, we have generated a method of correlating emitted blast waves with suppressive structure design

---

*The amount of oxygen available within any complete structure is unaffected by venting, until the venting area becomes very large.

based on comparing free-field blast data to blast data for waves emanating from suppressive structures. This method introduces an effective vent area ratio, α_{eff}, which can be computed for any combination of vented elements in a suppressive structure panel. Using this parameter and least-squares curve fits to free-field and suppressive structures blast data, we have shown that the influence of the suppressive structure is to create an effective standoff distance R_{sf}, less than the free-field standoff distance R_f at which side-on overpressure P_s is the same for a given blast source energy W. Alternatively, this method will predict the reduction in overpressure over a considerable range of distances outside the structure. Details of the method are also given later.

II. BLAST PRESSURES OUTSIDE SUPPRESSIVE STRUCTURES

The side-on overpressures P_s in the free-field around an explosive charge are given by a functional relationship as expressed in Eq. (1).

$$P_s = f\left(\frac{R}{W^{1/3}}\right) \qquad \text{(free field)} \qquad (1)$$

where

    R · standoff distance
    W – charge weight

This functional relationship is the famous Hopkinson blast scaling law for the blast field around geometrically similar sources at sea-level ambient atmospheric conditions.[3] Assume that a cubical blast suppressive structure whose length on any side is X and whose walls are fabricated of a single metal sheet with holes drilled in it is now centered over the explosive charge. The ratio of the vent area of a wall to the total presented area of the wall will be defined as equaling α. Equation (1) for free-field blast will now be modified by the additional geometric parameters defining the size of the suppressive cube X and the vent area ratio α. If we elect to write a modified form for Eq. (1) in nondimensional terms, a functional equation for predicting blast pressures outside the suppressive structure becomes:

$$P_s = f_1\left(\frac{R}{W^{1/3}}, \frac{X}{R}, \alpha\right) \qquad \text{(suppressive structure equation)} \qquad (2)$$

Equation (2) represents a four-parameter space of nondimensional numbers or pi terms. Although no functional format is expressed by Eq. (2), sufficient quantities of experimental data can be used to obtain an empirical relationship. This is precisely what is done to develop a relationship for predicting blast pressures outside of the suppressive structure; however, we must first realize that most suppressive structures do not have walls which are a single sheet with holes. The vast majority of structures have three to six wall layers with various staggered venting patterns so fragments will not escape the confinement. This means that, for

8

a multiwalled confinement, we must compute an effective α, α_{eff}, so Eq. (2) can be used to predict blast pressures. To compute α_{eff} for a multiwalled structure, we have assumed that:

$$\frac{1}{\alpha_{eff}} = \frac{1}{\alpha_1} + \frac{1}{\alpha_2} + \ldots + \frac{1}{\alpha_N} \tag{3a}$$

where N = number of elements in a suppressive structure panel. Or,

$$\frac{1}{\alpha_{eff}} = \sum_{i=1}^{i=N} \frac{1}{\alpha_i} \tag{3b}$$

Although no theoretical proof of this relationship is presently possible, it does reach the appropriate limits for small and large numbers of plates. For example, if only one plate is present, $\alpha_{eff} = \alpha_1$, as it should. If an infinite number of plates are present, $\alpha_{eff} = 0$, with the flow completely choked. If one of the plates is solid and thus has a zero α, $\alpha_{eff} = 0$, as it should. If all plates have the same value for α, $\alpha_{eff} = \alpha/N$, which is a number smaller than α for a single plate, as would be expected. In each member, α is defined according to Eq. (4).

$$\alpha = \frac{A_{vent}}{A_{wall}} \tag{4}$$

For plates, the meaning of this definition is obvious; however, in angles and louvres, the definition is less obvious. Figure 1 defines α in a series of angles.

In a louvre, we use a similar definition of α, except that the α, determined on the basis of Eq. (4), is multiplied by a factor equal to 1/2. This factor was applied because the data of Reference 12 indicate that louvres are more efficient in constricting flow than are plates with holes. Perhaps this is explained by the fact that the entrance of a louvre is perpendicular to the entrance of a hole in a wall. As will be shown later, the factor of 1/2 appears to be justified by a curve fit to the experimental data. Figure 2 illustrates our definition of α for a louvre.

Now that α_{eff} has been defined, we are prepared to develop a functional format for Eq. (2). This format was developed by assuming that Eq. (2) can be expressed as

$$P_s = A \left(\frac{R}{W^{1/3}}\right)^{N_1} \left(\frac{X}{R}\right)^{N_2} \left(\alpha_{eff}\right)^{N_3} \tag{5}$$

If logarithms are taken of both sides of this equation,

$$(\log P_s) = (\log A) + N_1 \left(\log \frac{R}{W^{1/3}}\right) + N_2 \left(\log \frac{X}{R}\right) + N_3 \left(\log \alpha_{eff}\right) \tag{6}$$
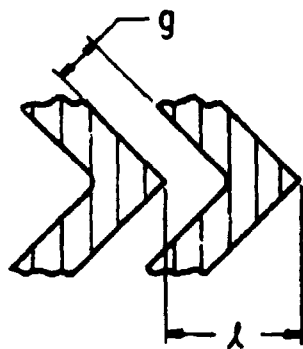
FIGURE 1. DEFINITION OF α IN A SERIES OF ANGLE MEMBERS

$$\alpha = \frac{g}{\lambda}$$
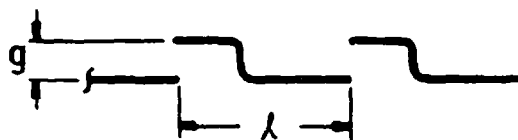
FIGURE 2. DEFINITION OF α IN A LOUVRE

$$\alpha = \frac{g}{2\lambda}$$

The equation is made linear, and a least-squares curve fit can be developed by stating that:

$$\left[1.0, \log \frac{R}{W^{1/3}}, \log \frac{X}{R}, \log \alpha_{eff} \right] \begin{bmatrix} \log A \\ N_1 \\ N_2 \\ N_3 \end{bmatrix} = [\log P_s] \tag{7}$$

Substituting matrix notation yields:

$$[L] \, [N] = [P] \tag{8}$$

and a least squares curve fit results for $\log A$, N_1, N_2, and N_3 or the N matrix when:

$$[N] = [L^T L]^{-1} \, [L^T] \, [P] \tag{9}$$

Experimental test data from References 9-12 were used to develop this curve fit. The resulting equation is

$$P_s = 976.3 \, \frac{W^{2/3} \alpha_{eff}^{1/2}}{R^{3/2} X^{1/2}} \tag{10}$$

10

where

P_s side-on pressure (psi)
W charge weight (lb)
R standoff distance from charge (ft)
X width of suppressive cube (ft)
α effective vented area ratio (-)

Figure 3 is a plot of Eq. (10) versus the experimental data points used to compose this plot. Equation (10) appears to fit the test results excellently. One standard deviation for the experimental data about the line in Figure 3 equals 18.6%, which is only slightly worse than would be obtained for free-field data. Because this is a curve fit to test data, Eq. (10) should only be used when input conditions fall within variations in individual pi terms. The variations included in test results were:

$$0.0263 \leqslant \alpha_{eff} \leqslant 0.60$$

$$0.323 \leqslant \frac{X}{R} \leqslant 1.77 \tag{11}$$

$$4.27 \text{ ft/lb}^{1/3} \leqslant \frac{R}{W^{1/3}} \leqslant 17.5 \text{ ft/lb}^{1/3}$$

The test data include results for a wide variety of panel geometries and numbers of vented layers in each panel. These range from as few as two layers to as many as five, and combinations of spaced angles, zees, perforated plates, and louvres.

It is interesting to curve fit free-field side-on blast pressure data from References 9-12 using the same procedure over the same range as for the suppressive structure blast field data. The resulting equation for free-field data is

$$P_s = 976.3 \left(\frac{W^{2/3}}{R^2} \right) \tag{12}$$

A comparison between Eq. (12) and the test data points can be seen in Figure 4. The standard deviation for blast pressures in the free-field is 13.1% which is only slightly better than the standard deviation for the suppressive structure blast field equation. Naturally, Eq. (12) should only be applied whenever $R/W^{1/3}$ is between the limits established by Eq. (11).

If one compares Eq. (10) for suppressive structures to Eq. (12) for free-field blast, it is immediately apparent that the influence of the suppressive structure is to create an effective standoff distance less than the free-field standoff distance at which blast pressures are the same for a given energy release. This standoff distance with a structure suppressing the blast R_{st} is related to the free-field standoff distance R_f by:
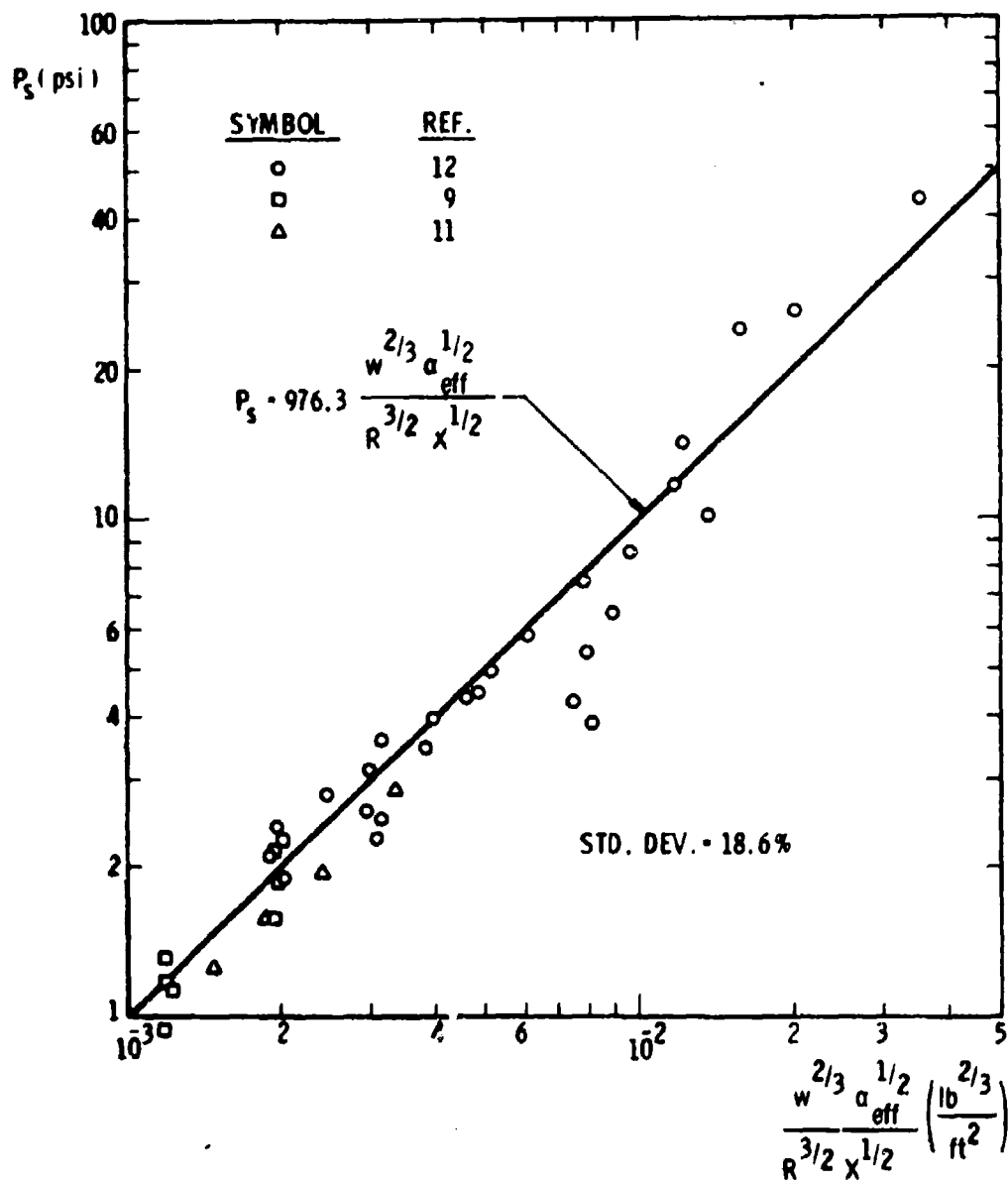
11

FIGURE 3. CURVE FIT TO BLAST PRESSURES OUTSIDE SUPPRESSIVE STRUCTURES

12

$$R_f^2 = R_{st}^{3/2} \frac{\chi^{1/2}}{\alpha_{eff}^{1/2}} \tag{13}$$

or

$$R_{st} = \alpha_{eff}^{1/3} \left(\frac{R_f^{4/3}}{\chi^{1/3}} \right) \tag{14}$$

III. PRESSURE RISE INSIDE STRUCTURE

In this section, we will discuss the quasi-static pressure rise within a suppressive structure. To create a solution, we will first perform a model analysis. The problem is envisioned as an instantaneous energy release of magnitude W inside a confined volume V. A vent area ($\alpha_{eff}A$) exists through which internal gases can escape. We are interested in predicting the internal pressure rise p and its decay as functions of time t. Ambient atmospheric pressure p_o exists initially inside and outside the confined volume. To define an equation of state for the gases in this problem, we need two additional parameters, the ratio of specific heats γ and speed of sound c_o. Table 1 summarizes the parameters in this problem and lists their fundamental dimensions in an engineering system of force, length and time (F, L, T).

Texts such as Reference 13 tell how nondimensional numbers or pi terms can be developed from this list of variables. Because no new assumptions are inserted in developing pi terms, we will present only the results and not perform all of the algebra. The assumptions in this analysis are all included in the definition of the problem, so that phenomena are not considered which have no parameter listed in Table 1. Probably the major assumption is that no thermal effects are considered; in other words, the pressures dissipate through the venting and not through the conduction of heat into walls of the suppressive structure, therefore an acceptable set of pi terms which can result is:

TABLE 1. PARAMETERS DETERMINING QUASI-STATIC PRESSURE INSIDE A VENTED CONTAINMENT VESSEL

Parameter	Symbol	Fundamental Dimensions	Description
Volume	V	L^3	Geometry
Vented Area	$(\alpha_{eff}A)$	L^2	Geometry
Energy Release	W	FL	Input energy
Atomospheric Pressure	p_o	F/L^2	Initial state of air
Sound Speed in Air	c_o	L/T	Initial state of air
Specific Heat Ratio Air	γ	—	Initial state of air
Pressure Increase	p	F/L^2	Response
Time	t	T	Response

$$\pi_1 = \frac{p}{p_o} \qquad \pi_2 = \frac{(\alpha_{eff}A)^{3/2}}{V} \qquad \pi_3 = \gamma$$

$$\pi_4 = \frac{W}{p_o V} \qquad \pi_5 = \frac{c_o t}{V^{1/3}} \tag{15}$$

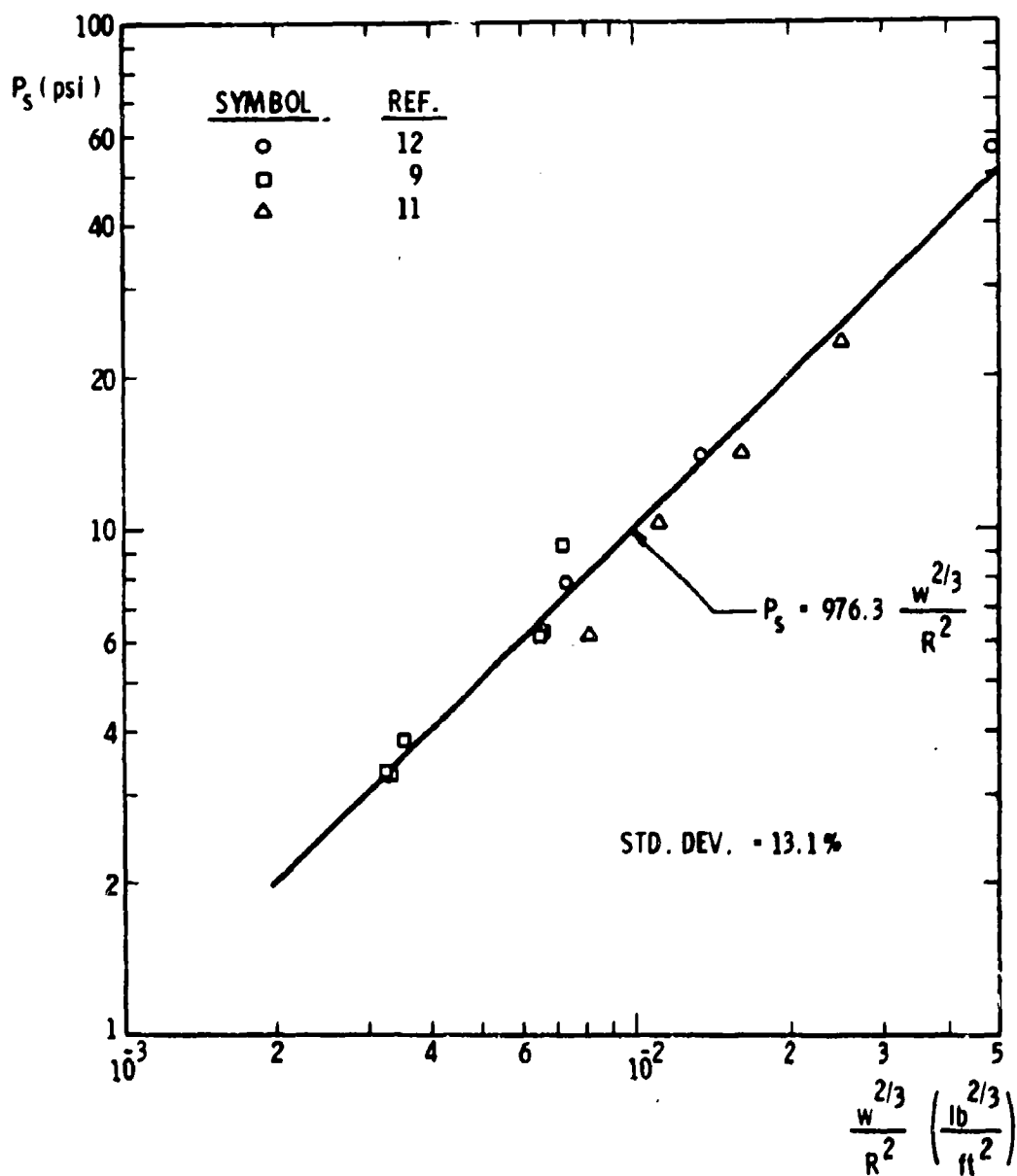If we assume γ is a constant and are only interested in predicting peak

FIGURE 4. CURVE FIT TO FREE FIELD BLAST PRESSURES

pressure, the result would not be dependent upon time or the pi terms π_3 and π_5 would be invariant. Hence,

$$\frac{p_{max}}{p_o} = f_1\left(\frac{W}{p_o V}, \frac{(\alpha_{eff}A)^{3/2}}{V}\right) \tag{16}$$

Because p_o is also invariant, we can write a dimensional functional format for Eq. (16).

$$p_{max} = f_2\left(\frac{W}{V}, \frac{(\alpha_{eff}A)^{3/2}}{V}\right) \tag{17}$$

Figure 5 is a plot of p_{max} versus W/V for various values of π_2. Provided π_2 is less than 0.0775, the experimental data indicate that the maximum pressure p_{max} is independent of $(\alpha_{eff}A)^{3/2}/V$. This can be written as

$$p_{max} = f_3\left(\frac{W}{V}\right), \quad \frac{(\alpha_{eff}A)^{3/2}}{V} \leqslant 0.0775 \tag{18}$$

The data used in developing Figure 5 come from References 7 and 8. In addition to presenting their own data which were obtained at the Naval Civil Engineering Laboratory, Keenan and Tancreto also report test data obtained by Proctor at the Naval Ordnance Laboratory. Both groups of experiments used Comp B explosive, but, as can be seen in Figure 5, their experiments were in different domains of W/V.

The dashed straight lines in Figure 5 are the asymptotes for complete energy conversion or for p_{max} proportional to (W/V). If (W/V) is too large, insufficient oxygen is available to convert all the energy in the explosive charge; hence, the energy release is reduced by the ratio of the heat of detonation divided by the heat of combustion. Figure 5 implies that for $W/V \leqslant 0.003$ complete oxidation occurs; for $W/V \geqslant 0.1$, the only oxidizer available is that in the explosive itself, and W/V between 0.003 and 0.1 results in partial afterburning.

If the maximum pressure is reached before significant venting occurs, the blow-down time will be independent of π_4, and we can write a functional equation for time of blow-down.

$$\frac{c_o t}{V^{1/3}} = f_4\left(\frac{p}{p_o}, \frac{(\alpha_{eff}A)^{3/2}}{V}\right) \tag{19}$$

Neglecting the invariant ambient gas parameters in Eq. (19) permits us to write a dimensional form of Eq. (19).

$$\frac{t}{V^{1/3}} = f_5\left(p, \frac{(\alpha_{eff}A)^{3/2}}{V}\right) \tag{20}$$
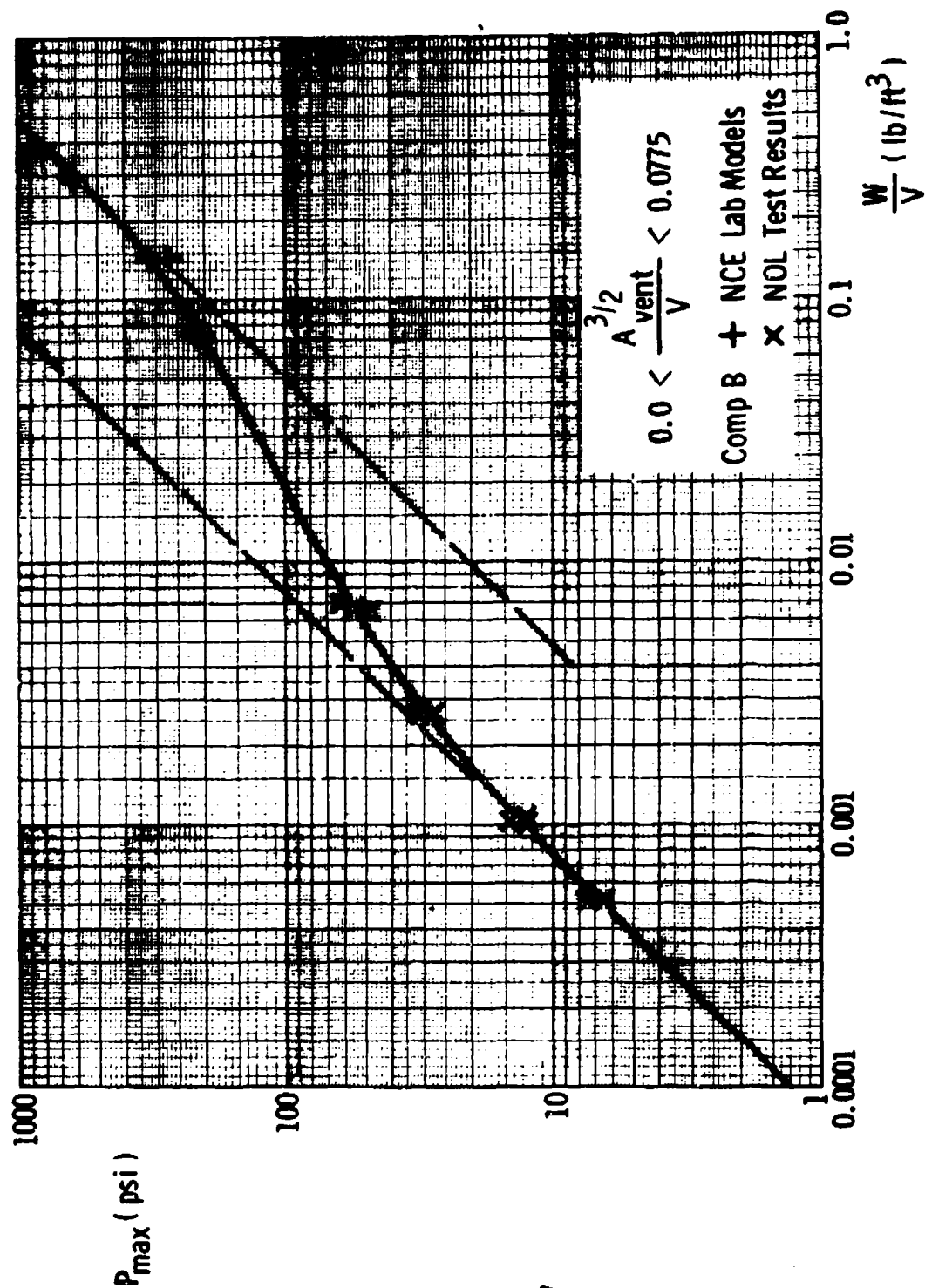
FIGURE 5. QUASI-STATIC PRESSURE RISE INSIDE AN UNVENTED ENCLOSURE

The data used to develop Figure 5 can also be used to empirically solve Eq. (20). Figure 6 is a plot of $t/(p^{1/6} V^{1/3})$ versus $(\alpha_{eff} A)^{3/2}/V$. The ordinate of this graph is based on the empirical observation that the two pi terms $t/V^{1/3}$ and p can be combined to from $t/(p^{1/6} V^{1/3})$. We can now write Eq. (20) as Eq. (21):

$$\frac{t}{p^{1/6} V^{1/3}} = f_6 \left(\frac{(\alpha_{eff} A)^{3/2}}{V} \right) \qquad (21)$$

The functional format for Eq. (21) is obtained from Figure 6.

IV. CONCLUSIONS AND RECOMMENDATIONS

In this report, we have presented methods for estimating long term (quasi-static) pressures generated by internal explosions within vented suppressive structures, and attenuated blast pressures escaping from suppressive structures with various vent panel design. Scaled curves for appropriate parameters are presented, based on fits to available experimental data.

We have several suggest ons for improving methods for estimating blast loading and attenuation of suppressive structures:

(1) Initial reflected blast loads have conservatively been estimated to be the reflected pressures and impulses on rigid, non-vented walls. We suggest that shock-tube or field tests be conducted to measure these loads more accurately, for several typical vent panel designs.

(2) Experimental data for quasi-static pressure rises caused by internal explosions in vented structures have been limited to such small values of scaled vent areas that the maximum pressure rises are unaffected by the vent areas. Tests should be run on well-vented structures to determine scaled vent areas which which cause significant reduction in quasi-static pressures.

(3) As additional data on attenuated blast pressures outside suppressive structures are obtained in the course of subsequent testing, these data should be factored into the design curves and equations in this report to obtain better fits. In addition, curve fits should be made to scaled data for blast impulse outside the structures, when sufficient data are available.

REFERENCES

1. H. J. Goodman, "Compiled Free-Air Data on Bare Spherical Pentolite," BRL Report No. 1092, Ballistic Research Laboratories, Aberdeen Proving Ground, Md., Feb. 1960 (AD 235-278).
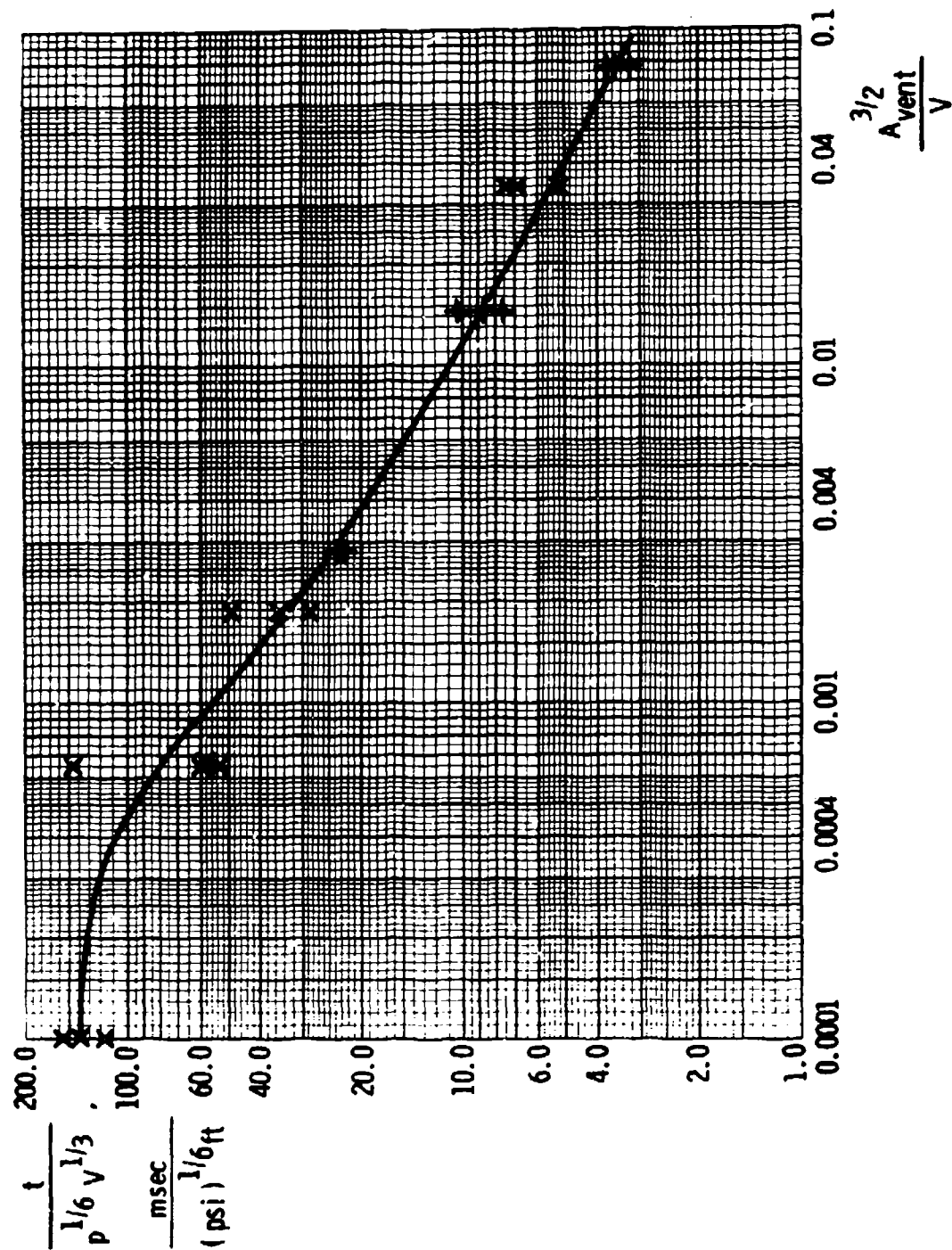
FIGURE 6. SCALED BLOW-DOWN TIME FOR VENTED STRUCTURE.

2. W. H. Jack, Jr., "Measurements of Normally Reflected Shock Waves from Explosive Charges," BRL Memorandum Report No. 1499, Ballistic Research Laboratories, Aberdeen Proving Ground, Md., 1963.

3. W. E. Baker, Explosions in Air Univ. of Texas Press, Austin, Texas, 1973.

4. J. F. Proctor and W. S. Filler, "A Computerized Technique for Blast Loads from Confined Explosions," 14th Annual Explosives Safety Seminar, New Orleans, La., 8-10 Nov. 1972, pp. 99-124.

5. J. F. Proctor, "Internal Blast Damage Mechanisms Computer Program," 61 jTCG/ ME-73-3, Joint Technical Coordinating Group for Munitions Effectiveness, 10 April 1973.

6. R. G. S. Sewell and G. F. Kinney, "Internal Explosions in Vented and Unvented Chambers," 14th Annual Explosives Safety Seminar, New Orleans, La., 8-10 Nov. 1972, pp. 87-98.

7. W. A. Keenan and J. E. Tancreto, "Effects of Venting and Frangibility on Blast Environment from Explosions in Cubicles," Minutes of the Fourteenth Explosives Safety Seminar, New Orleans, Nov. 1973, pp. 125-:61.

8. W. A. Keenan and J. E. Tancreto, "Blast Environment from Fully and Partially Vented Explosions in Cubicles," Tech. Rept. 51-027, Civil Engineering Laboratory, Naval Construction Battalion Center, Port Hueneme, Ca., Feb. 1974.

9. A. H. Lasseigne, "Static and Blast Pressure Investigation for the Chemical Agent Munition Demilitarization System: Sub-Scale," Rept. EA-FR-4C04, Nov. 30, 1S73.

10. Report EA1002, "Study of Suppressive Structures Applications to an 81 mm Automated Assembly Facility," prepared for Manufacturing Technology Directorate, Chemical and Plants Division, Edgewood Arsenal, 16 April 1973.

11. Report EA-4E33, "81 mm Suppressive Shielding Technical Data Package," Jan. 1974.

12. Report EA-FR-2B02, "Final Report Application of Suppressive Structure Concepts to Chemical Agent Munition Demilitarization System (CAMDS)," July 27, 1973.

13. W. E. Baker, P. S. Westine and F. T. Dodge, Similarity Methods in Engineering Dynamics, Hayden Book Co., Inc., Rochelle Park, N. J., 1973.

DISTRIBUTION OF SUPPRESSIVE SHIELDING REPORTS

Addressee	No. of Copies
Commander Rocket Propulsion Laboratory Attn: Mr. M. Raleigh Edwards Air Force Base, CA 93523	1
Commander HQ, Armament Development Test Center Attn: DOM/Mr. S. Reither Eglin Air Force Base, FL 32542	1
Commander Hill Air Force Base Attn: MMNTR/Mr. Cummings Clearfield, UT 84406	1
Commander Norton Air Force Base Attn: AFISC-SEV/Mr. K. Collinsworth San Bernardino, CA 92409	1
Commander Air Force Civil Engineering Center Attn: AFCEC-DE/LTC Walkup Tyndall Air Force Base Panama City, FL 32401	1
Commander HQ Air Force Logistics Command Attn: MMWM/CPT D. Rideout IGYE/Mr. K. Shopher Wright-Patterson Air Force Base Dayton, OH 45433	1 ea
Commander Naval Ordnance Systems Command Attn: Code ORD 43B/Mr. A. Fernandes Washington, DC 20360	1
Commander Explosives Safety Attn: ADTC/SEV (Mr. Ron Allen) Eglin Air Force Base, FL 32542	1

Commander   1 ea
US Army Materiel Command
Attn: AMCCG
        AMCRD/Dr. Kaufman
        AMCSF/Mr. W. Queen
        AMCPM-CS/COL Morris
5001 Eisenhower Ave.
Alexandria, VA 22333

Office of the Project Manager for   3
Munition Production Base Modernization
   and Expansion
Attn: AMCPM-PBM-E/Mr. Dybacki
USA Materiel Command
Dover, NJ 07801

Commander   1 ea
US Army Armament Command
Attn: AMSAR-EN/Mr. Ambrosini
        AMSAR-SC/Dr. C. Hudson
        AMSAR-SF/Mr. J. Varcho
        AMSAR-TM/Mr. Serlin, Mr. T. Fetter, Mr. S. Porter
        AMSAR-MT/Mr. A. Madsen, Mr. G. Cowan, CPT Burnsteel
Rock Island Arsenal
Rock Island, IL 61201

Commander   1 ea
USAMC Ammunition Center
Attn: Mr. J. Byrd
        AMXAC-DEM/Mr. Huddleston
                    Mr. Sumpterer
Savanna, IL 61074

Commander   1 ea
Frankford Arsenal
Attn: Mr. F. Fidel, Mr. E. Rempler
Bridge and Tacony Sts.
Philadelphia, PA 19137

Commander
Picatinny Arsenal
Attn: Mr. Saffian   3
        Mr. J. Cannovan   1 ea
        Mr. Hickerson
        Mr. I. Forsten
Dover, NJ 07801

Commander   1
USA Test and Evaluation Command
Attn: AMSTE-NB
Aberdeen Proving Ground, MD 21005

Commander   1 ea
Dugway Proving Ground
Attn: Dr. Rothenburg
        Mr. P. Miller
Dugway, UT 84022

Commander   1
Cornhusker Army Ammunition Plant
Grand Island, NE 68801

Commander   1
Indiana Army Ammunition Plant
Charleston, IN 47111

Commander   1
Iowa Army Ammunition Plant
Burlington, IA 52502

Commander   1
Joliet Army Ammunition Plant
Joliet, IL 60436

Commander   1
Kansas Army Ammunition Plant
Parsons, KS 67357

Commander   1
Longhorn Army Ammunition Plant
Marshall, TX 75671

Commander   1
Lone Star Army Ammunition Plant
Texarkana, TX 75502

Commander   1
Louisiana Army Ammunition Plant
Shreveport, LA 71102

Commander   1
Milan Army Ammunition Plant
Milan, TN 38358

Commander   1
Radford Army Ammunition Plant
Radford, VA 24141

Commander   1
Sunflower Army Ammunition Plant
Lawrence, KS 66044

Commander   1
Lake City Army Ammunition Plant
Attn: Mr. John Jacobi
Independence, MO 64056

Commander   1
Ravenna Army Ammunition Plant
Ravenna, OH 44266

Commander   1
Pine Bluff Arsenal
Pine Bluff, AR 71601

Director
US Army Materiel Systems Analysis Activity
Aberdeen Proving Ground, MD 21005

Director   5
US Army Ballistics Research Laboratories
Attn: Mr. R. Vitali
Aberdeen Proving Ground, MD 21005

Division Engineer   1 ea
US Army Engineer Division, Huntsville
Attn: HNDED-R/Mr. Dembo
                    Mr. W. Char
P.O. Box 1600, West Station
Huntsville, AL 35807

US Army Engineer Division   1
Waterways Experimental Station
P.O. Box 631
Vicksburg, MS 39180

Director   1
USAMC Intern Training Center
Attn: Dr. G. Chiang
Red River Depot
Texarkana, TX 75502

Dr. Robert D. Siewert   1
NASA Lewis Laboratory
21000 Brook Park Rd
Cleveland, OH 44135

Mr. George Pinkas   1
Code 21-4
NASA Lewis Laboratory
21000 Brook Park Rd
Cleveland, OH 44135

Mr. W. H. Jackson   1
Deputy Manager for Engineering
Atomic Energy Commission
P.O. Box E
Oak Ridge, TN 37830

Mr. Erskine Harton   1
US Department of Transportation
Washington, DC 20315

Dr. Jean Foster   1
US Department of Transportation
Washington, DC 20315

Mr. Frank Neff   1
Mound Laboratory
Monsanto Research Corp.
Miamisburg, OH 45342

Ms. Trudy Prugh   1
Mound Laboratory
Monsanto Research Corp.
Miamisburg, OH 45342

Commander   1
Naval Weapons Laboratory
Attn: Mr. F. Sanches
Dahlgren, VA 22448

Dr. W. E. Baker   1
Southwest Research Institute
San Antonio, TX 78284

Division Engineer   1
US Army Engineer Division, Fort Belvoir
Fort Belvoir, VA 22060

Commander   1
Naval Sea Systems Command
Washington, DC 20315

Mr. Billings Brown   1
Hercules, Inc.
Box 98
Magna, UT 84044

Mr. John Komos   1
Defense Supply Agency
Cameron Station
Alexandria, VA 22030

Office of the Project Manager for Chemical   2
  Demilitarization and Installation Restoration
Edgewood Arsenal
Aberdeen Proving Ground, MD 21010

Edgewood Arsenal
Technical Director
Attn: SAREA-TD-E   1
Foreign Intelligence Officer   1
Chief, Legal Office   1
Chief, Safety Office   1
CDR, US Army Technical Escort Center   1
Author's Copy, Manufacturing Technology Directorate   3
Aberdeen Proving Ground, MD 21010

Edgewood Arsenal
Director of Biomedical Laboratory
Attn: SAREA-BL-M   1
       SAREA-BL-B   1
       SAREA-BL-E   1
       SAREA-BL-H   1
       SAREA-BL-R   1
       SAREA-BL-T   1
Aberdeen Proving Ground, MD 21010

Edgewood Arsenal
Director of Chemical Laboratory
Attn: SAREA-CL-C   1
       SAREA-CL-P
Aberdeen Proving Ground, MD 21010

Edgewood Arsenal
Director of Development & Engineering
Attn: SAREA-DE-S   4
Aberdeen Proving Ground, MD 21010

Edgewood Arsenal
Director of Manufacturing Technology
Attn: SAREA-MT-TS 2
       SAREA-MT-M   1
Aberdeen Proving Ground, MD 21010

Edgewood Arsenal
Director of Product Assurance
Attn: SAREA-PA-A   1
       SAREA-PA-P   1
       SAREA-PA-Q   1
Aberdeen Proving Ground, MD 21010

Edgewood Arsenal
Director of Technical Support
Attn: SAREA-TS-R   2
       SAREA-TS-L   3
       SAREA-TS-E   1
Aberdeen Proving Ground, MD 21010

Aberdeen Proving Ground   1
Record Copy
CDR, APG
Attn: STEAP-AD-R/RHA
APG-Edgewood Area, BLDG E5179
Aberdeen Proving Ground, MD 21005

Aberdeen Proving Ground   1
CDR, APG
Attn: STEAP-TL
APG, Aberdeen Area
Aberdeen Proving Ground, MD 21005

DEPARTMENT OF DEFENSE
Administrator   12
Defense Documentation Center
Attn: Accessions Division
Cameron Station
Alexandria, \ 22314

Commander
Edgewood Arsenal   1
Attn: SAREA-DM
Aberdeen Proving Ground, MD 21010